The Journal of Experimental Biology 207, 285-293
Published by The Company of Biologists 2004
doi:10.1242/jeb.00746

Are melanized feather barbs stronger?

Michael Butler and Amy S. Johnson*

Biology Department, 6500 College Station, Bowdoin College, Brunswick, ME 04011, USA

*Author for correspondence (e-mail: ajohnson@bowdoin.edu)

Accepted 8 October 2003

Summary

Melanin has been associated with increased resistance to abrasion, decreased wear and lowered barb breakage in feathers. But, this association was inferred without considering barb position along the rachis as a potentially confounding variable. We examined the cross-sectional area, breaking force, breaking stress, breaking strain and toughness of melanized and unmelanized barbs along the entire rachis of a primary feather from an osprey (*Pandion haliaetus*). Although breaking force was higher for melanized barbs, breaking stress (force divided by cross-sectional area) was greater for unmelanized barbs. But when position was considered, all mechanical differences between melanized and unmelanized barbs disappeared. Barb breaking stress, breaking strain and toughness decreased, and breaking stiffness increased, distally along the rachis. These proximal–distal material property changes are small and seem unlikely to affect flight performance of barbs. Our observations of barb bending, breaking and morphology, however, lead us to propose a design principle for barbs. We propose that, by being thicker-walled dorso-ventrally, the barb's flexural stiffness is increased during flight; but, by allowing for twisting when loaded with dangerously high forces, barbs firstly avoid failure by bending and secondly avoid complete failure by buckling rather than rupturing.

Key words: barb, feather, strength, biomechanics, melanin, color, material properties.

Introduction

In addition to functions such as signaling and counter shading, feather color is thought to play a mechanical role. For example, an increase in melanin is associated with a reduction of feather wear due to abrasion (Burtt, 1979, 1986; reviewed in Bonser, 1996). It follows that melanin is more likely to be found in feathers more exposed to wear, such as those in the wing tips of gulls or gannets (Gill, 1995). Decreased feather surface area and length was observed on the albino side of a partially albino yellow-rumped warbler (*Dendroica coronara auduboni*; Barrowclough and Sibley, 1980). Similarly, white spots on barn swallow (*Hirundo rustica*) wings showed more breakage than was expected by chance (Kose and Møller, 1999). Furthermore, increased wear was seen in an albino greater shearwater (*Puffinus gravis*), resulting in lower wing area, lower maneuverability and slower speed than pigmented conspecifics (Lee and Grant, 1986).

Few studies, however, have tested for mechanical differences between melanized and unmelanized keratin. Several studies have shown a correlation between increased melanin and abrasion resistance (Burtt, 1979, 1986; Barrowclough and Sibley, 1980; Lee and Grant, 1986; Kose and Møller, 1999). Bonser and Witter (1993) found that the keratin of melanized European starling (*Sturnus vulgaris*) bills had a significantly higher Vickers hardness than did unmelanized bill keratin. Similarly, Bonser (1995) found that melanized feather keratin of the willow ptarmigan (*Lagopus lagopus* race *scoticus*) had a higher Vickers hardness than did unmelanized feather keratin. In the behavioral literature, strength and hardness have been equated (Fitzpatrick, 1998), despite any direct experimental evidence linking the two. Perhaps they are related because in the center of feather keratin is a large crystalline region (Greg and Rogers 1984, cited in Vincent, 1990), and in crystals tensile strength is a maximum of one-third its Vickers hardness (Vincent, 1990). Thus, greater hardness sometimes implies greater tensile strength. Although a direct linkage between hardness and breaking has not been established for feather barbs, Burtt (1986) quantified a direct melanin-related effect on breakage. In that study, abrasion was simulated by small glass beads blown at feathers by an air stream; a smaller fraction of melanized barbs than unmelanized barbs were broken.

Differences in melanin, however, might be associated with other factors of biomechanical importance, confounding the comparisons cited above. It has been suggested, for example, that melanin is associated with thickening of the structure of the outer, cortical layer of the feather keratin *via* deposition of melanoprotein granules (see Burtt, 1986 for a review). Such thickening affects the cross-sectional morphology, which will affect derived mechanical parameters such as breaking stress. Indeed, cross-sectional morphology was found to affect flexural stiffness of the rachises of eight species (Bonser and Purslow, 1995). In addition, it is possible, indeed likely, that

color will be non-randomly distributed with respect to both cross-sectional area and position on feathers.

To assess the contribution of barb morphology and position to mechanical performance, we quantify cross-sectional area, breaking force, breaking stress, breaking strain and toughness of melanized and unmelanized barbs along the entire rachis of a primary feather from an osprey (*Pandion haliaetus*).

Materials and methods

Test specimen

A primary feather was obtained from the frozen right wing of an osprey (*Pandion haliaetus* L.). The feather was asymmetrical (as most flight feathers are), with the smaller side (leading edge) being mostly dark gray or black, and the larger side (trailing edge) having white and dark bands running perpendicular to the rachis. Barbs on the trailing edge of the feather were assigned a number (n), with 1 at the most proximal end and 302 at the most distal end. There were more barbs distal to 302, but they were too short for experimentation. The barbs were cut at a distance ranging between 5 mm and 10 mm from the rachis, with each sample 15–20 mm long. Fractional distance (*d*) along the rachis was calculated by dividing the barb number (n) by the total number of barbs (302) in the experimental region of the feather. Barbs that were not fully black or white were discarded, leading to a grouping of data points of monochromatic barbs between gaps in the data due to bicolored barbs. The lack of black proximal and white distal data points is due to the impurity of colors in these regions.

Mechanical tests

Each feather barb was mounted in a materials testing device such that the initial length between the screw-and-nut grips was 9–15 mm. The specimen was extended at 8 mm min^{-1} until breakage. Force was measured using a strain-gage-based force beam (error, less than ±0.02 N), and extension was measured using a linear variable differential transformer or LVDT (error, less than ±0.004 mm). Data were digitized (12-bit) at 100 Hz. Relevant mechanical variables were calculated from the force extension curve, the initial length and the cross-sectional area. The initial length was measured using calipers (error, less than ±0.01 mm) as the distance between the grips at zero load.

Grips at each end consisted of a screw with two nuts. The feather barb was inserted through one nut; the screw, which already had one nut threaded onto it, was then screwed onto the nut while the feather barb was in the nut. The nut already on the screw was tightened against the nut containing the feather barb. In this way, the barb was held in place by the corrugations of the screw and nut. By microscopic examination, it was possible to determine that there was no slippage at the grips because the screw threads caused permanent crimps of the barb inside the nut. The crimps corresponded to the screw threads. Breakage usually did not occur at the grips, indicating that the grips did not act to concentrate force at the ends of the test length.

We used tensile rather than bending tests because of the simplicity of determining breaking stresses with such tests. Previous research had shown that the rachis of pigeon flight feathers failed by buckling during four-point bending (Corning and Biewener, 1998). We initially tried bending 10 mm lengths of feather barbs but, because they are relatively slender (40–400 μm diameter) compared with pigeon feather rachis, our specimens bent into U-shapes before buckling. Such extreme bends made four-point bending tests impractical.

Cross-sectional area and wall thickness

The cross-section, height and width of each barb were measured at the broken end *via* scanning electron microscopy (SEM) and NIH image analysis software. To do this, the 3 mm closest to the broken end of each barb was snipped off, mounted on an SEM stub and carbon-coated. Digital photographs, including scales superimposed by the SEM software, were taken of the snipped end of each barb. Each cross-section was typically oval to rectangular and consisted of a solid cortex surrounding a foam-like medullary space (Fig. 1). To obtain barb cross-sectional areas, the outer and inner boundaries of the cortex were traced, yielding the cross-sectional area of the entire barb, s_o, and the cross-sectional area of the medullary space, s_m. By subtracting the area of the space from the area of the entire barb, we calculated the cross-sectional area of the cortex wall, s_c.

Although feather barbs are almost never cylindrical (see Fig. 1), for comparison with previous work (Corning and Biewener, 1998; Brazier, 1927; Alexander, 1996) we calculated the ratio of wall thickness to mean radius, $t/\bar{r}$, assuming a cylindrical shape. For a hollow cylinder with outer radius r_o and inner radius r_i, $t=r_o-r_i$ and $\bar{r}=(r_o-r_i)/2$. In terms of area, $r_o=\sqrt{a_o/\pi}$, where a_o is the cross-sectional area inside the outer edge of the cylinder. Similarly, $r_i=\sqrt{a_i/\pi}$, where a_i is the cross-sectional area of the hollow region. Combining the equations immediately above, the ratio of thickness to mean radius is:

$$\frac{t}{\bar{r}} = \frac{2(\sqrt{a_o}-\sqrt{a_i})}{\sqrt{a_o}+\sqrt{a_i}} . \quad (1)$$

(Note that in the equivalent formula in Corning and Biewener, 1998, their equation 2 contains a typographical error.) For estimating $t/\bar{r}$ of the feather barbs, we substituted s_o for a_o and s_m for a_i.

Calculated mechanical variables

Breaking stress, σ_{brk}, was defined as breaking force, F_{brk}, divided by s_c. Breaking strain, ε_{brk}, was calculated by dividing the breaking extension, l_{brk}, by the original length, l_o, of the barb test section. Work to break, W_{brk}, was determined by integrating the area under the force–extension curve. Toughness, *T*, or work per volume, was calculated by $W_{brk}/(s_c l_o)$.

Statistical tests

Factorial analysis of variance (ANOVA) was used to test

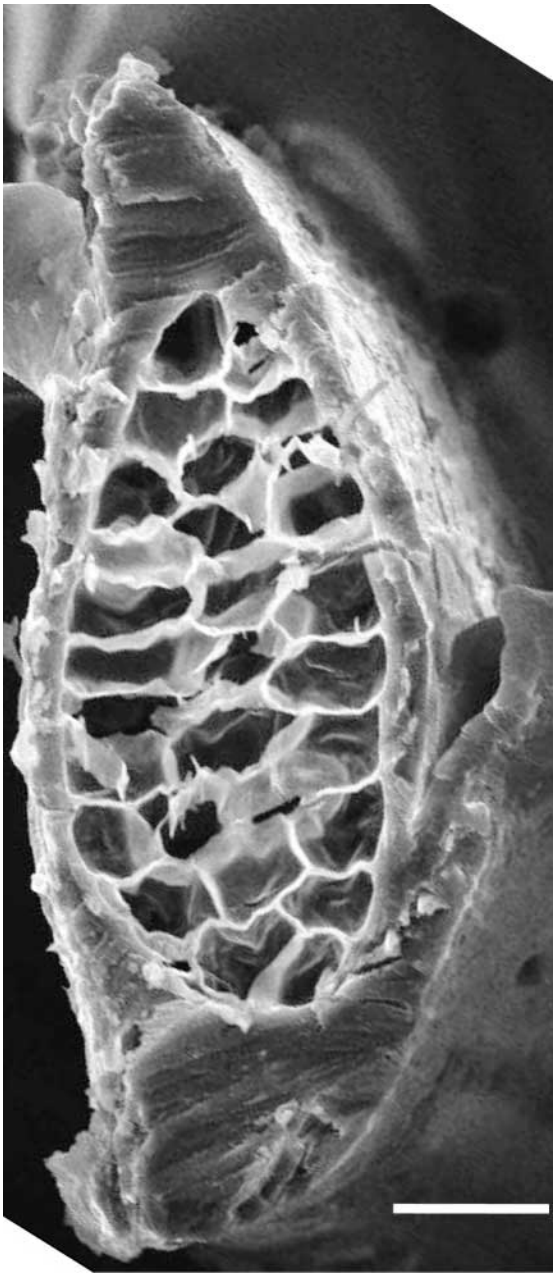

Fig. 1. An SEM photograph of the cross-section of one feather barb included in this study (fractional distance=0.63). Barb sections are typically rectangular to oval, almost always with the dorso-ventral axis (up–down in this photograph) longer and thicker walled than the lateral axis (right–left in this photograph). Scale bar, 30 μm.

for differences between breaking force and breaking stress of melanized and unmelanized barbs. Analyses of covariance (ANCOVA) were used with either d or ε_{brk} as covariates. ANCOVA formulas were from Zar (1996) and were used to test whether standard least squares linear regression lines for the classified variables were parallel (i.e. do the variables covary at the same rate). If significant differences among slopes were not found, then lines were tested to seek differences in elevations. When there were no differences

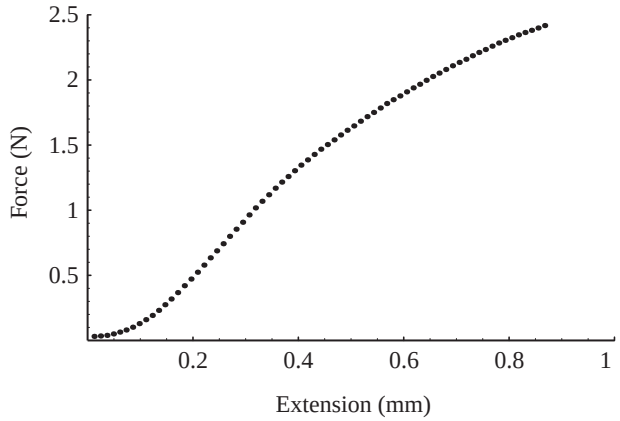

Fig. 2. An example of a force–extension curve of a feather barb extended at 8 mm min^{-1} until breakage. Data points were initially sampled at 100 Hz, but data points shown were resampled at 10 Hz for presentation. Mean values for mechanical variables are given in Table 1.

in either slopes or intercepts, the common slope and common intercept were used to plot the least squares regression lines.

Results

An example of an experimental plot of force *versus* extension of a feather barb shows an initial J-shaped curve, then a linear region, then a yield point followed by breakage (Fig. 2). Such a force–extension curve is consistent with the known structure of feather keratin. Specifically, feather keratin is a β-pleated sheet, which is an extended form of α-helical keratin. The force–extension curve for our feathers (β-keratin) thus resembles the most extended portion of the stress–extension curve for wool (α-keratin; compare with p. 190, Wainwright et al., 1976).

Summary statistics for relevant mechanical variables at breakage are given in Table 1 for all barbs that we measured. Values for breaking stress are similar to another keratin-based material, wool, which breaks at ~200–300 MN m^{-2} (Peter and Woods, 1955, cited in Wainwright et al., 1976; Hearle et al. 1971, cited in Vincent, 1990). Our values for breaking strains average 0.06, identical with that reported for feather keratin by Astbury and Woods (1933, cited in Vincent, 1990). Our values

Table 1. *Summary of breaking data for the feather barbs*

Variable	Mean	S.D.	S.E.M.	*N*
Force (F_{brk}) (N)	1.15	0.56	0.042	176
Extension (l_{brk}) (mm)	0.61	0.23	0.017	176
Stress (σ_{brk}) (MN m^{-2})	281	76	6.1	156
Strain (ε_{brk})	0.060	0.024	0.0018	176
Toughness (T) (MJ m^{-3})	10.1	6.7	0.54	156

Data for unmelanized and melanized barbs are pooled since no colour-based differences were detected (see figures and text).

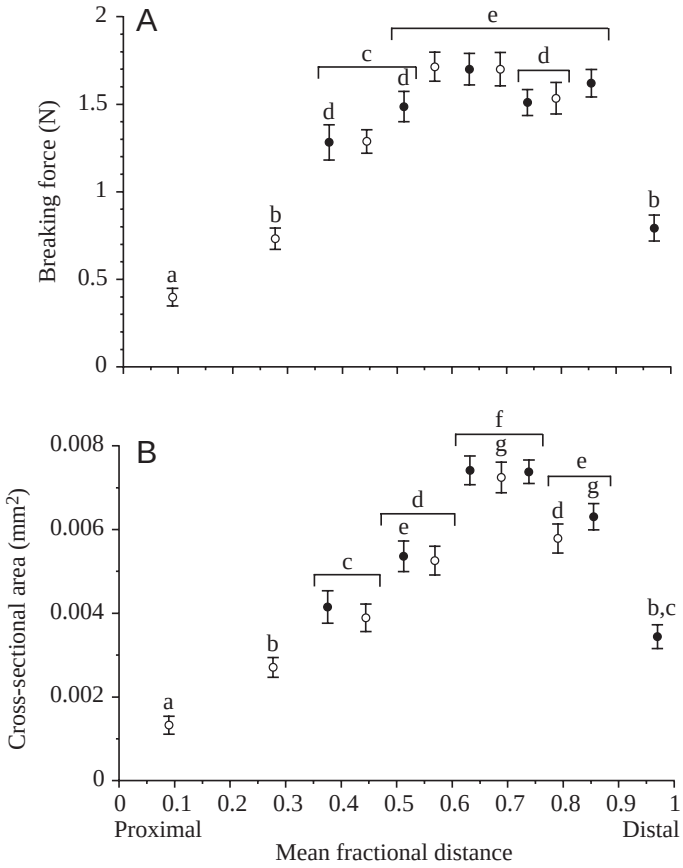

Fig. 3. Mean breaking force (A) and mean cross-sectional area (B) of unmelanized (open circles) and melanized (closed circles) bands of barbs as a function of mean fractional distance along the feather, where '0' represents the proximal end and '1' represents the distal end of the feather. Breaking force and cross-sectional area differed significantly between bands (ANOVA, $P<0.001$). Mean values for bands sharing the same letter were not significantly different (*a posteriori*; $P>0.05$); mean values for all other bands were significantly different.

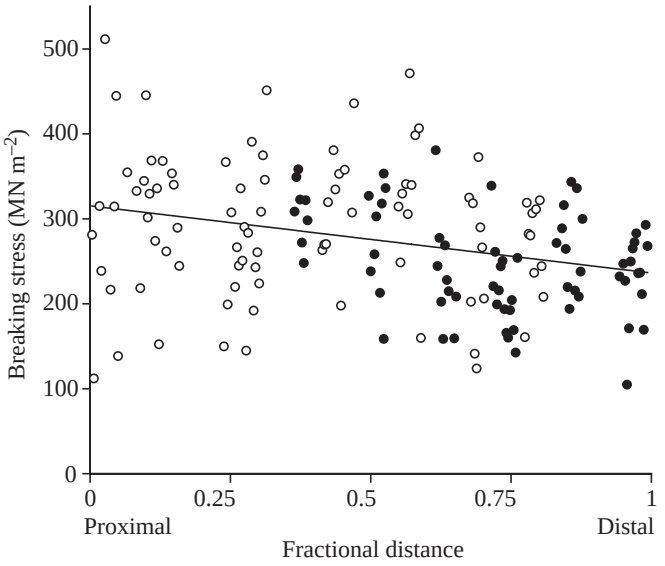

Fig. 4. Breaking stress (σ_{brk}) as a function of fractional distance (d) along the feather, where '0' represents the proximal end and '1' represents the distal end of the feather. There were no significant differences in slope (ANCOVA; $P_{2,153}=0.17$) or intercept ($P_{2,153}=0.09$) between barb colors (overall equation: $\sigma_{brk}=-79d+320$, $r^2=0.09$, $P_{1,154}<0.001$ that the overall slope is zero).

for toughness (10.1 MJ m^{-3}) are slightly lower than values given for keratin-based materials (15–30 MJ m^{-3}) on p. 185 in Denny (1988). Those keratin-based values are probably for wool, an α-keratin that probably has higher toughness because of the increased strain at breakage.

The breaking force of barbs increased as a function of increasing fractional distance from the proximal end of the feather, with a force plateau between fractional distances of 0.51 and 0.85 (Fig. 3A). Within this plateau, and in the three color bands just proximal to it, adjacent bands of different color typically did not differ in breaking force. The two most proximal bands and the most distal band all showed a significantly lower breaking force than all other bands. Similarly, cross-sectional area increased initially as a function of increasing distance and was least for the most proximal and distal bands (Fig. 3B). However, the cross-sectional area plateau was narrower and shifted more distally than the breaking force plateau.

ANOVA indicated overall that the breaking force of melanized barbs (1.38±0.06 N, mean ± S.E.M.) was greater than that of unmelanized barbs (1.00±0.05 N; $P_{1,174}<0.001$). Similarly, overall the cross-sectional area of melanized barbs ($5.70\times10^{-3}\pm0.26\times10^{-3}$ mm^2) was greater than that of unmelanized barbs ($3.56\times10^{-3}\pm0.23\times10^{-3}$ mm^2; $P_{1,154}<0.001$).

However, when breaking force was normalized for cross-sectional area (i.e. breaking stress was calculated), ANOVA indicated that the breaking stress of unmelanized barbs (292.7±7.9 MN m^{-2}) was greater than that of melanized barbs (249.4±8.9 MN m^{-2}; $P_{1,154}<0.001$). When we took into account the position of the barbs on the feathers, regressions

Table 2. *Summary of morphological measurements for the feather barbs*

Variable	Mean	S.D.	S.E.M.
Cortical cross-sectional area (s_c) (mm^2)	0.0045	0.0024	0.00019
Medullary cross-sectional area (s_m) (mm^2)	0.0041	0.0027	0.00022
s_m/s_c (=k_a)	0.87	0.17	0.014
Thickness/mean radius ($t/\bar{r}$)	0.39	0.057	0.0046
Mean height (μm)	166	76.5	6.13
Mean width (μm)	66.8	16.0	1.28

Data for unmelanized and melanized barbs are pooled. Thickness/mean radius ratio assumes that the barbs have a hypothetical hollow cylindrical shape. Height is in the dorso–ventral direction; width is in the lateral direction. $N=156$ for all measurements.

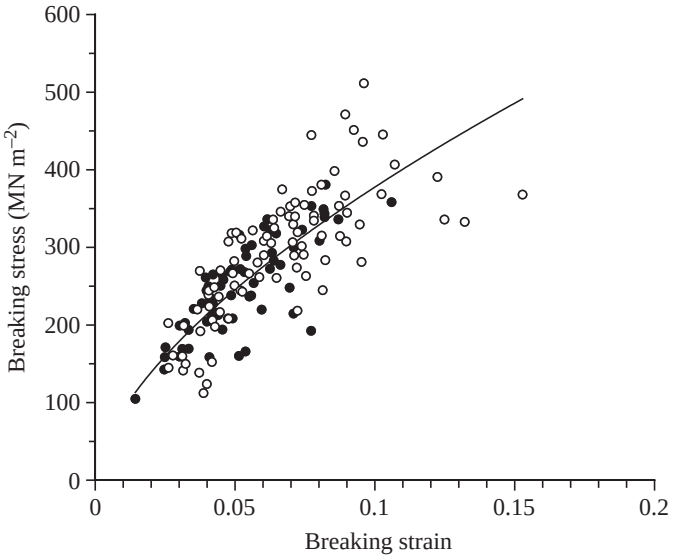

Fig. 5. Power fit of breaking stress (σ_{brk}) as a function of breaking strain (ε_{brk}) of the unmelanized (open circles) and melanized (closed circles) barbs. There were no significant differences in slope (ANCOVA; $P_{2,153}$=0.42) or intercept ($P_{2,153}$=0.74) between barb colors for the log-transformed data (overall equation: $\sigma_{brk}=1600\varepsilon_{brk}^{0.62}$, r^2=0.66, $P_{1,154}$<0.001 that the overall slope is zero).

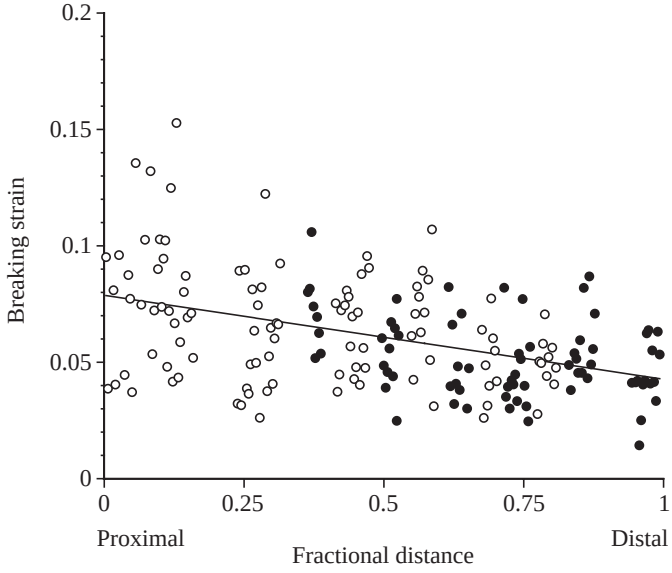

Fig. 7. Breaking strain (ε_{brk}) as a function of fractional distance (d) along the feather, where '0' represents the proximal end and '1' represents the distal end of the feather. There were no significant differences in slope ($P_{2,153}$=0.78) or intercept ($P_{2,153}$=0.52) for each barb color (overall equation: $\varepsilon_{brk}=-0.036d+0.079$, r^2=0.19, $P_{1,154}$<0.001 that the overall slope is zero).

of breaking stress as a function of fractional distance along the feather were best fit by a one-slope, one-intercept model (Fig. 4; statistics reported in figure legend). Thus, strength was independent of barb color when position along the rachis was taken into account. Breaking stress of barbs decreased from the proximal to the distal end of the feather.

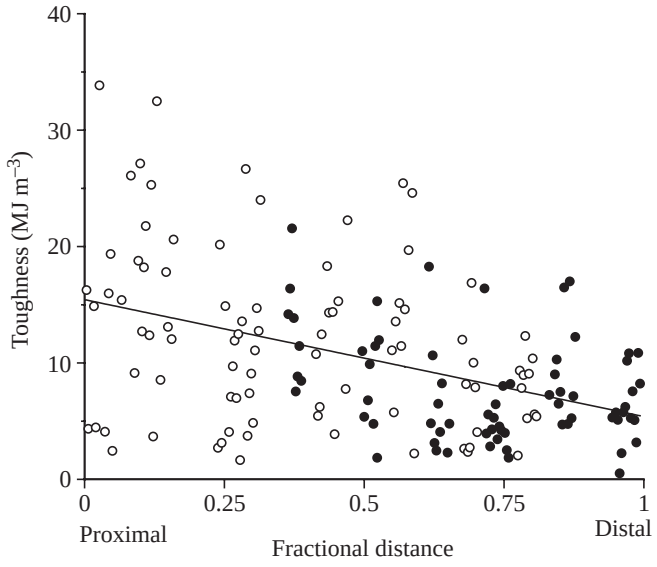

Fig. 6. Toughness (T) as a function of fractional distance (d) along the feather, where '0' represents the proximal end and '1' represents the distal end of the feather. There were no significant differences in slope ($P_{2,153}$=0.76) or intercept ($P_{2,153}$=0.22) between barb colors (overall equation: $T=-10d+15$, r^2=0.19, $P_{1,154}$<0.001 that the overall slope is zero).

To assess the causes of this pattern of breaking stress, one needs to consider the possible contribution of the medullary foam. The relevant variable is the ratio of the medullary cross-sectional area to cortex cross-sectional area, s_m/s_c. This ratio increases linearly from 0.48 at the most proximal end to 1.2 at a fractional distance of 0.88 and then decreases to 0.43 for barbs at the most distal end of the rachis (mean ± S.E.M., 0.87±0.014; Table 2). In the Discussion, we consider whether the medullary foam contributes to the observed patterns of breaking stress.

The breaking stress did increase as a function of increasing strain, with no significant difference in this relationship between the two barb colors (Fig. 5; statistics reported in the figure legend).

Both toughness (Fig. 6) and breaking strain (Fig. 7) decreased as a function of fractional distance, with no difference between the slope or intercept for melanized and unmelanized barbs (statistics reported in the figure legends).

For comparison with data available in the literature on feather rachis, and because the behavior of beams is affected by their cross-sectional shape, a summary of measured morphological variables is given in Table 2.

Discussion

Are melanized feather barbs stronger?

While greater abrasion resistance of melanized *versus* unmelanized keratin has been frequently reported (see

Introduction), other morphological differences (such as cross-sectional area) or positional differences (such as location along the rachis of a feather) that might confound these results have not typically been assessed. We found that while apparent mechanical differences between melanized *versus* unmelanized barbs did occur, these differences disappeared when morphology and position of the barbs were also taken into account. Thus, understanding the mechanical characteristics associated with feather color entails taking into account differences in measured force not only as a function of color but also as a function of barb morphology and position.

We did find that if only color was taken into account then the breaking force of melanized barbs was significantly greater than that of unmelanized barbs, which is consistent with reports from the literature (see Introduction). However, this difference was less compelling when mean breaking force for each color band was plotted as a function of fractional distance from the distal end of the feather (Fig. 3A). Adjacent bands in the middle of the feather tended to have the same breaking force, independent of the color of the band. Similarly, bands of opposite color on either end of the feather were more similar in breaking force to each other than they were to bands in the middle of the feather.

This positional pattern of breaking force was associated with a similar positional pattern in barb cross-sectional area (Fig. 3B). Cross-sectional area largely determined differences in breaking force between barbs. Thus, the plateaus of breaking force and cross-sectional area both occur at similar points along the feather, with lower values at the more extreme ends of the feather. When we normalized breaking force for cross-sectional area (i.e. calculated breaking stress), without taking into account position, however, the breaking stress of unmelanized barbs was actually significantly greater than that of melanized barbs. When position of the barbs along the feather was taken into account as well (Fig. 4), there was no longer any significant difference in the strength of melanized *versus* unmelanized barbs. Thus, the strength of unmelanized barbs was higher not because of intrinsic strength differences associated with melanin but because there were more of them located in a stronger (proximal) location. Position entirely explained the strength differences among barbs.

The absence of material property differences that could be attributed to melanization is also apparent when breaking stress is analyzed as a function of breaking strain (Fig. 5). Similarly, toughness (Fig. 6) and breaking strain (Fig. 7) of barbs was not different for melanized *versus* unmelanized barbs when these variables were considered as a function of fractional distance. Thus, material properties of barbs did not depend on melanin.

It has been suggested that melanization serves to increase hardness by inducing thickening of the tegument (see Introduction), thereby increasing cross-sectional area. In Fig. 3B, we can compare cross-sectional area of adjacent differently colored bands. In five of nine such comparisons, there were no differences in cross-sectional area. In the four comparisons where significant differences were detected, the melanized barbs always had higher cross-sectional area. This lends at least speculative support to the possibility that melanin might slightly increase cross-sectional area and hardness. Mainly, however, the pattern of variation indicates the necessity of careful sampling design to tease apart positional effects from possible melanin-induced effects.

Does the strength of barb cortex decrease distally along the rachis?

Our estimate of barb cortical strength assumed no contribution from the medullary material; could a systematically changing contribution of the medullary material explain the apparent distal decrease in cortical strength? It can be shown, as follows, that if the relative stiffness of the medulla is 1% of that of the cortex (Bonser, 1996) then the overestimate of strength is between 0.4% and 1.2%, depending on the proportion of total cross-sectional area that consists of medulla. To see this, consider that a barb is a structure with two materials that contribute to the total tensile breaking force, $F=F_c+F_m$, where F_c and F_m are the breaking force of the cortical and medullary materials, respectively. The structure fails at a strain, ε, and the forces due to the cortex and medulla are $F_c=E_c s_c \varepsilon$ and $F_m=E_m s_m \varepsilon$, respectively, where E_c and E_m are the Young's moduli of the cortex and medulla, respectively. Let the modulus of one material be a multiple of the modulus of the other material, $E_m=k_E E_c$, with a constant k_E, and let the cross-sectional area of one material be a multiple of the other area, $s_m=k_a s_c$, with a constant k_a. We estimated cortical strength by dividing the total force by the cortical area. To the degree that the medullary material contributes to the total force, cortical strength will be overestimated. We can calculate the factor by which the cortical strength is overestimated by dividing the estimated strength by the hypothetical strength, combining the equations above:

$$\frac{F/s_c}{F_c/s_c} = 1 + k_a k_E \,. \qquad (2)$$

For the feather barbs in this study, k_a averages 0.87 (Table 2) and ranges between 0.43 and 1.2; Bonser (1996) quantified the stiffness of rachis medulla as 1% of the stiffness of the cortex such that $k_E=0.01$. Thus, the range of values for $(F/s_c)/(F_c/s_c)$ are 1.0043 to 1.012, which indicates that the variability in estimated cortical strength due to the contribution of the medullary material is ~1%. Such a small contribution of the medulla is unlikely to account for the observed 25% decrease in estimated cortical strength at the most distal positions along the rachis. Furthermore, the ratio of medullary cross-sectional area to total cross-sectional area of barbs increased with distance along the rachis up to a fractional distance of 0.88, which is in the opposite direction needed to explain a decrease in estimated cortical strength due to differential contribution of the medulla. So, changes in the contribution of the medullary material cannot explain the decrease in cortical strength that we observed. The observed decrease in strength of barbs towards the distal end of the rachis must be due to changes in the material properties of the cortex keratin.

Material property changes with position along the rachis

have been previously observed for feather cortex keratin. For example, the stiffness of the cortex keratin from the rachis of mute swan (*Cygnus olor*) flight feathers has been shown to increase by 100% from the proximal to the distal end of the rachis (Bonser and Purslow, 1995). If we calculate a nominal breaking stiffness as breaking stress over breaking strain, we find that there is a 37% increase in nominal breaking stiffness of barbs located towards the distal end of the rachis. Thus, the cortex of both rachis and barbs increases in stiffness towards the distal end of the rachis. Such location-dependent material property changes in stiffness, strength, breaking strain and toughness should be incorporated into studies of feather structure and function.

Do material property changes of the more distal barbs affect flight performance?

A small decrease in material strength of the barbs towards the distal end of the rachis is unlikely to contribute much to differential function of barbs during flight. This is because barbs are normally loaded in bending during flight. The bending performance of barbs will be controlled by their flexural stiffness, which is the product of stiffness (a material property) and the second moment of area (a measure of the distribution of cortex material around the neutral axis in the plane of bending). Bonser and Purslow (1995) concluded that the flexural stiffness of the primary feathers of the mute swan was principally controlled by the second moment of area, despite a 100% increase in stiffness along the rachis. Similarly, the consequences to bending performance of changes in the second moment of area that occur in barbs along the length of the rachis are likely to overwhelm the consequences of small changes in material properties of those barbs.

Does bending performance of barbs differ from that of the rachis?

When bent to failure (buckling), the deflection of barbs is relatively much greater than that of the rachis. This phenomenon is perhaps best understood in terms of the radius of curvature at failure. The radius of curvature (ρ) in a bent beam is:

$$\rho = \frac{Ez}{\sigma_z}\ , \qquad (3)$$

where E is the Young's modulus, z is the distance from the neutral axis towards the outer margin of the beam, and σ_z is the stress in the bent beam at z (Wainwright et al., 1976). We use the same values for Young's modulus and tensile failure stress as did Corning and Biewener (1998), originally obtained from the literature (Bonser and Purslow, 1995; Crenshaw 1980, cited in Corning and Biewener, 1998) to calculate the radius of curvature as a function of the height (in the plane of bending), h, of the bending structure. If $E=2.5\times10^9$, the tensile rupture stress is $\sigma_z=226\times10^6$ and $z=h/2$, then

$$\rho = 5.5h\ . \qquad (4)$$

We use the tensile rupture stress as a reference point even though both rachis and barbs fail by buckling. We do this because the buckling stress is not known and changes systematically with the wall thickness. As cylindrical beams become thicker walled, the buckling moment becomes equal to the moment at tensile rupture. We are interested here in evaluating mainly the effect of the relative slenderness of the beam and the relative curvature at failure. Thus, we use as a single reference point the tensile failure stress and acknowledge that in both barbs and feathers the buckling failure will occur at a somewhat variable lower value of stress and curvature.

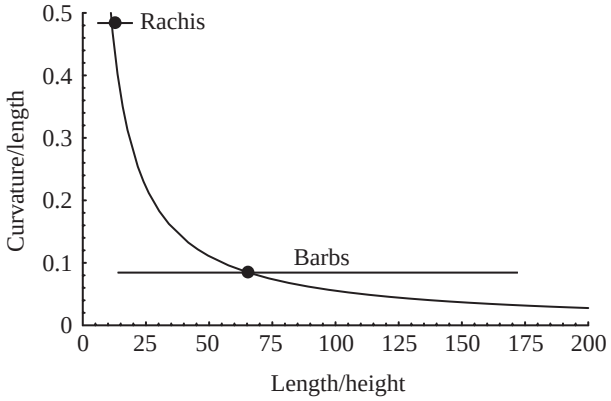

Fig. 8. The relative curvature of a bent beam at failure as a function of the slenderness of the beam. The relative curvature is given by the radius of curvature at failure (ρ evaluated as in Equation 4) divided by the length of the beam (L) plotted against the length divided by the height of the beam (L/h). Averages (dots) and ranges of values (horizontal lines) shown are for the osprey feather tested in the current experiment. Barbs deform much more relative to their length before failing by buckling than does the rachis of a feather. Thus, barbs avoid failure by bending, whereas the rachis avoids failure by depending more on structural and material strength.

We define relative curvature as the radius of curvature at failure divided by the length of the beam, ρ/L, and we define slenderness as the ratio, L/h, of a beam's length to its effective height (where effective height is the dimension perpendicular to the length but in the plane of bending). These two dimensionless numbers can be plotted against each other (Fig. 8), such that the typical range of slenderness values is shown for the feather rachis and barbs used in this study. At failure, barbs are relatively much more curved than the rachis. Thus, barbs tend to avoid buckling failure by bending out of the way of high forces, whereas the rachis is less able to bend sufficiently to avoid high forces.

This effect of slenderness on flexibility is enhanced in the barbs because they twist as they bend. Barbs are typically taller than wide (Fig. 1; Table 2), but when they twist, the smaller dimension, the width, becomes the effective height, thus lowering the second moment of area and allowing a smaller radius of curvature before reaching a critical buckling stress. The tendency to twist has also been observed to a lesser degree in the rachis of pigeon flight feathers (Corning and Biewener, 1998). In barbs, twisting persists even when groups of barbs

are tested, despite the increase in lateral stability provided by such groups (M.B. and A.S.J., personal observation).

Thus, if you assume that cortex keratin of barbs and rachis buckles at the same stress, a smaller radius of curvature will be observed for the barbs at that stress than will be observed for the rachis. For feather rachis, the stress for buckling is less than the tensile rupture stress (Corning and Biewener, 1998), and buckling can generally be expected in thin-walled beams (Brazier, 1927). But as the wall gets thicker, the buckling and rupture moments converge. Whereas the pigeon rachis was thin walled ($t/\bar{r}$=0.081±0.0078; Corning and Biewener, 1998), the osprey barbs were relatively thicker walled ($t/\bar{r}$=0.39±0.0046; Table 2). The barbs will therefore be likely to have a higher buckling stress, a stress approaching that predicted by the tensile rupture of feather keratin.

One can estimate the relative wall thickness at which a beam should fail in tensile rupture rather than in buckling. This calculation is done using the equation for buckling moment (equation 4 in Corning and Biewener, 1998), the equation for the rupture moment (a rearrangement of equation 6 in Corning and Biewener, 1998; not their equation 3, which contains a typographical error) and the definition $r_i=\kappa_r r_o$, where κ_r is the ratio of inner to outer radii. Then, using the same values for Young's modulus, tensile failure stress, constant K and Poisson's ratio as did Corning and Biewener (1998), the ratio of inner to outer radii at which the buckling moment equals the rupture moment is κ_r=0.81. The ratio κ_r is related to the $t/\bar{r}$ ratio by the following formula:

$$\frac{t}{\bar{r}} = \frac{2(1-\kappa_r)}{(1+\kappa_r)}\ ; \qquad (5)$$

thus, when κ_r=0.81, $t/\bar{r}$=0.21. A higher $t/\bar{r}$ (=0.39) for barbs predicts that the barbs should fail in tensile rupture.

In contrast to this prediction, we observed that bent barbs failed in buckling. Buckling presumably occurred because the barbs twist during bending and the wall thickness in the plane of bending after this twisting is considerably less than the mean wall thickness of the barb. [See Fig. 1 to understand a change in the plane of bending due to twisting; bending dorso-ventrally (up–down in Fig. 1) becomes lateral bending after twisting.] It may be that twisting partly functions to prevent failure by tensile rupture, which would probably be more catastrophic to barb function than is buckling. Buckling usually leaves an intact but weakened barb and therefore a barb that still functions almost as well as before buckling. We propose the following design principle for barbs. By being thicker-walled dorso-ventrally (see Fig. 1), their flexural stiffness is increased during flight; but by allowing for twisting when loaded with dangerously high forces they firstly avoid failure by bending and secondly avoid complete failure by buckling rather than rupturing.

High flexibility and deformability may function to prevent breakage in barbs, as it does in other systems. For instance, daffodil stems, which have low torsional stiffness, twist to reduce drag in wind (Etnier and Vogel, 2000). Similarly, flexibility in terebellid polychaete tentacles (which deform; Johnson, 1993) and stipes of kelp (which bend; Johnson and Koehl, 1994) also functions to reduce drag. Finally, extreme extensibility in viscid spider silk (Denny, 1976) and mussel byssal threads (Bell and Gosline, 1996) functions to avoid high forces by allowing deformation.

The role of melanin in signaling feather quality

Theories about the role of bird plumage in signaling feather quality (Fitzpatrick, 1998) rest critically on whether feather coloration accurately reflects mechanical properties of the feather. To the extent that feather coloration is unimportant to the mechanical function of feathers, it suggests that patterns of melanized and unmelanized feather coloration evolved under selective pressures, such as communication, counter-shading or thermoregulation, different from those involved in the mechanical function of feathers. It may be that the preference of feather-eating lice for unmelanized regions of feathers compromises feather strength in some species of birds (Kose and Møller, 1999), and, perhaps, unbroken feathers with large white spots signal the absence of feather-eating lice. However, while dark and light bar patterns may indeed aid the perception of the extent of wear and damage, the corollary that the absence of melanin facilitates feather wear needs to be examined more rigorously.

Summary

Whereas our measurements of material properties on one feather from one species cannot determine whether melanization contributes to strength or hardness in bird species in general, our discovery of the importance of position to material properties calls into question previous results in which positional effects were not considered. Sampling of the tissues to be tested must involve careful experimental design of the sampling scheme to adequately account for effects of location and cross-sectional area. Such sampling must be undertaken before it can be concluded that melanization functions to increase hardness, toughness or strength of keratin-based structures in birds.

List of symbols

a_i	cross-sectional area of the hollow region inside the wall
a_o	cross-sectional area inside the outer wall edge
d	fractional distance of the barb along the rachis
E	Young's modulus
E_c	Young's modulus of the cortex
E_m	Young's modulus of the medulla
F_{brk}	total breaking force
F_c	breaking force of the cortex material
F_m	breaking force of the medullary material
h	height in the plane of bending
K	constant in equation 4 in Corning and Biewener (1998)
k_a	ratio of medullary to cortex area
k_e	ratio of medullary to cortex Young's modulus

L	length of the beam
l_{brk}	breaking extension
l_o	original length of the barb test section
n	barb number
$\bar{r}$	mean wall radius
ρ	radius of curvature
r_i	inner wall radius
r_o	outer wall radius
s_c	cross-sectional area of the cortex
s_m	cross-sectional area of the medulla
s_o	cross-sectional area of the entire barb
T	toughness
t	wall thickness
W_{brk}	work to break
z	distance from the neutral axis towards the outer margin of the beam
ε_{brk}	breaking strain
κ_r	ratio of inner to outer radii
σ_{brk}	breaking stress
σ_z	stress in the bent beam at z

This work was supported by grants to A.S.J. from the Kenan Foundation and the Whitehall Foundation. We thank C. K. Field for technical assistance with the SEM, and O. Ellers for technical assistance with the mechanical testing apparatus, assistance in development of theory and comments on the manuscript. We also thank N. Wheelwright for discussions and for providing osprey feathers from the Bowdoin College bird collection, and two anonymous reviewers for comments on the manuscript.

References

Alexander, R. McN. (1996). *Optima for animals.* Revised edition. Princeton: Princeton University Press.

Barrowclough, G. F. and Sibley, F. C. (1980). Feather pigmentation and abrasion: test of a hypothesis. *Auk* **97**, 881-883.

Bell, E. C. and Gosline, J. M. (1996). Mechanical design of mussel byssus: material yield enhances attachment strength. *J. Exp. Biol.* **199**, 1005-1017.

Bonser, R. H. C. (1995). Melanin and the abrasion resistance of feathers. *Condor* **97**, 590-591.

Bonser, R. H. C. (1996). The mechanical properties of feather keratin. *J. Zool. Lond.* **239**, 477-484.

Bonser, R. H. C. and Purslow, P. P. (1995). The Young's modulus of feather keratin. *J. Exp. Biol.* **198**, 1029-1033.

Bonser, R. H. C. and Witter, M. S. (1993). Indentation hardness of the bill keratin of the European starling. *Condor* **95**, 736-738.

Brazier, L. G. (1927). On the flexure of thin cylindrical shells and other "thin" sections. *Proc. R. Soc. Lond. Ser. A* **116**, 104-114.

Burtt, E. H., Jr (1979). Tips on wings and other things. In *The Behavioral Significance of Colour* (ed. E. H. Burtt, Jr), pp. 75-125. New York: Garland STPM Press.

Burtt, E. H., Jr (1986). An analysis of physical, physiological and optical aspects of avian colouration with emphasis on wood-warblers. *Ornithol. Monogr.* **38**, 1-126.

Corning, W. R. and Biewener, A. A. (1998). *In vivo* strains in pigeon flight feather shafts: implications for structural design. *J. Exp. Biol.* **201**, 3057-3065.

Denny, M. W. (1976). The physical properties of spider's silk and their role in the design of orb webs. *J. Exp. Biol.* **65**, 483-506.

Denny, M. W. (1988). *Biology and the Mechanics of the Wave-Swept Environment.* Princeton: Princeton University Press.

Etnier, S. A. and Vogel, S. (2000). Reorientation of daffodil (Narcissus: Amaryllidaceae) flowers in wind: drag reduction and torsional flexibility. *Am. J. Bot.* **87**, 29-32.

Fitzpatrick, S. (1998). Birds' tails as signaling devices: markings, shape, length, and feather quality. *Am. Nat.* **151**, 157-173.

Gill, F. B. (1995). Feathers. In *Ornithology* (ed. F. B. Gill), pp. 65-92. New York: W. H. Freeman and Co.

Johnson, A. S. (1993). Sag-mediated modulated tension in terebellid tentacles exposed to flow. *Biol. Bull.* **185**, 10-19.

Johnson, A. S. and Koehl, M. A. R. (1994). Maintenance of environmental stress factor in different flow habitats: thallus allometry and material properties of a giant kelp. *J. Exp. Biol.* **195**, 381-410.

Kose, M. and Møller, A. P. (1999). Sexual selection, feather breakage and parasites: the importance of white spots in the tail of the barn swallow (*Hirundo rustica*). *Behav. Ecol. Sociobiol.* **45**, 430-436.

Lee, D. S. and Grant, G. S. (1986). An albino greater shearwater: feather abrasion and flight energetics. *Wilson Bull.* **98**, 488-490.

Vincent, J. (1990). *Structural Biomaterials*. Princeton: Princeton University Press.

Wainwright, S. A., Biggs, W. D., Currey, J. D. and Gosline, J. M. (1976). *Mechanical Design in Organisms.* Princeton: Princeton University Press.

Zar, J. H. (1996). *Biostatistical Analysis*. Third edition. New Jersey: Prentice–Hall.